JPEDAV (2016) 37:672–679
DOI: 10.1007/s11669-016-0495-6
1547-7037 ©ASM International

Measurement of 900 °C Isothermal Section in the Mo-Ni-Zr System

Shimin Wang, Cong Zhang, Chaoying Lin, Yingbiao Peng, and Yong Du

(Submitted June 28, 2016; in revised form July 23, 2016; published online August 23, 2016)

The isothermal section of the Mo-Ni-Zr system at 900 °C was investigated by characterization of eighteen equilibrium alloys. Electron probe microanalysis (EPMA) and x-ray diffraction (XRD) were used to identify the phases and obtain their compositions. The existence of two ternary compounds, $Zr_{65}Mo_{18-x}Ni_{16.5+x}$ (τ_1, cF96-Ti_2Ni) and $Zr_{65}Mo_{27.3}Ni_{7.7}$ (τ_2, hP28-Hf_9Mo_4B), was confirmed in the Zr-rich corner, and the compositions of the two phases were determined. The isothermal section of the Mo-Ni-Zr system at 900 °C consists of 15 three-phase regions and 29 two-phase regions. The following three-phase equilibria were well established: (1) (Ni) + Ni_7Zr_2 + Ni_5Zr, (2) MoNi + $MoNi_3$ + Ni_7Zr_2, (3) Ni_7Zr_2 + MoNi + (Mo), (4) (Mo) + Ni_7Zr_2 + Ni_3Zr, (5) (Mo) + Ni_3Zr + $Ni_{21}Zr_8$, (6) (Mo) + $Ni_{21}Zr_8$ + $Ni_{10}Zr_7$, (7) (Mo) + $Ni_{10}Zr_7$ + NiZr, (8) (Mo) + Mo_2Zr + NiZr, (9) $NiZr_2$ + Mo_2Zr + τ_1, (10) τ_1 + Mo_2Zr + τ_2, (11) τ_2 + Mo_2Zr + (Zr)ht, (12) $NiZr_2$ + τ_1 + (Zr)ht and (13) τ_1 + τ_2 + (Zr)ht. Several binary phases, such as $MoNi_3$, Ni_7Zr_2 and Mo_2Zr, dissolve appreciable amount of the third component.

Keywords electron probe microanalysis, Mo-Ni-Zr, microstructure, phase equilibria, x-ray diffraction

1. Introduction

Ti(C,N)-based cermets have been widely used as cutting tool materials owing to their excellent wear resistance, high-temperature hardness, well chemical stability, low friction coefficient to metals, and superior thermal deformation resistance.[1,2] The addition of Mo or Mo_2C into cermets can improve the wettability between ceramic phase and binder phase, and the cermets with finer microstructure and better mechanical properties can be obtained.[3] The addition of ZrC into cermets can improve its toughness and thermal shock resistance,[4,5] while Ni is an important binder metal for Ti(C,N)-based cermets. In addition, the Ni-Zr binary system has been widely investigated as an important metallic glass system. Recently, Yang et al.[6] found that the appropriate addition of Mo can stabilize an ordered structure of metallic glass with a higher atomic packing density and lower energy state, and it can also improve the glass formation ability of Mo-Ni-Zr alloys.

In this paper, to facilitate reading, the symbols to denote the stable phases in the Mo-Ni-Zr ternary system are summarized in Table 1.[7–9]

Shimin Wang, Cong Zhang, Chaoying Lin, and **Yong Du**, State Key Laboratory of Powder Metallurgy, Central South University, Changsha 410083 Hunan, People's Republic of China; and Sino-German Microstructure Cooperation Group, Central South University, Changsha 410083 Hunan, People's Republic of China; **Yingbiao Peng**, School of Metallurgical Engineering, Hunan University of Technology, Zhuzhou 412008 Hunan, People's Republic of China. Contact e-mail: yong-du@csu.edu.cn.

The binary phase diagrams used in the present work are briefly described as follows. The Ni-Zr binary system was recently assessed by Tokunaga et al.[10] and it shows the existence of eight intermediate phases: Ni_5Zr, Ni_7Zr_2, Ni_3Zr, $Ni_{21}Zr_8$, $Ni_{10}Zr_7$, $Ni_{11}Zr_9$, NiZr and $NiZr_2$. Except for Ni_3Zr phase, which is formed through a peritectoid reaction $Ni_7Zr_2 + Ni_{21}Zr_8 \leftrightarrow Ni_3Zr$, the formation of the other phases is associated with the liquid phase. The Ni_7Zr_2, NiZr and $NiZr_2$ phases melt congruently, while the Ni_5Zr, $Ni_{21}Zr_8$, $Ni_{11}Zr_9$ and $Ni_{10}Zr_7$ phases melt peritectically. The Ni-Zr phase diagram assessed by Tokunaga et al.[10] is shown in Fig. 1(a). The Mo-Ni binary system assessed by Santhy et al.[11] shows the presence of three intermetallic compounds: MoNi, $MoNi_3$ and $MoNi_4$. The MoNi phase is formed through a peritectic reaction L + (Mo) ↔ MoNi and the other two phases are formed through peritectoid reactions MoNi + (Ni) ↔ $MoNi_3$ and $MoNi_3$ + (Ni) ↔ $MoNi_4$. The eutectic reaction L ↔ MoNi + (Ni) occurs in the Ni-rich part of this binary system. The Mo-Ni phase diagram assessed by Santhy et al.[11] is shown in Fig. 1(b). The stable compound in the Mo-Zr system is Mo_2Zr, which melts peritectically.[12] The Mo-Zr phase diagram assessed by Jerlerud et al.[12] is shown in Fig. 1(c).

The Mo-Ni-Zr system was previously reviewed by Gupta[13] and the phase equilibria determinations have been carried out mainly by Virkar et al.[14] and Prima et al.[15–17] Their investigations[14–17] on the Mo-Ni-Zr system were performed in the entire composition region at 900 °C. Nevertheless, there are several contradictions among their work: (1) Virkar et al.[14] reported the presence of three ternary intermediate phases, Zr_4MoNi, Zr_9Mo_4Ni and $Zr_{33.3}Mo_3Ni_{63.7}$. However, only the Zr_4MoNi ternary phase was found by Prima et al.[15–17] Thus the existence of the ternary phases Zr_9Mo_4Ni and $Zr_{33.3}Mo_3Ni_{63.7}$ was questionable and required further confirmation; (2) in the Ni-rich corner, the $MoNi_3$ phase was found to be in equilibrium

Table 1 Crystal structure data for binary and ternary compounds in the Mo-Ni-Zr system at 900°C[15–17]

Phase	Structure type	Pearson symbol	Space group	Ref
(Mo)	W	cI2	Im-3 m	7
MoNi	$Mo_3(Mo_{0.8}Ni_{0.2})_5Ni_6$	oP56	$P2_12_12_1$	7
$MoNi_3$	Cu_3Ti	oP8	Pmmn	7
Mo_2Zr	$MgCu_2$	cF24	Fd-3 m	7
$NiZr_2$	$CuAl_2$	tI12	I4/mcm	7
NiZr	T_1I	oS8	Cmcm	7
$Ni_{10}Zr_7$	Zr_7Ni_{10}	oS68	Cmce	7
$Ni_{21}Zr_8$	Hf_8Ni_{21}	aP29	P-1	7
Ni_3Zr	Mg_3Cd	hP8	$P6_3/mmc$	7
Ni_7Zr_2	Zr_2Ni_7	mS36	C12/m1	7
Ni_5Zr	Be_5Au	cF24	F-43 m	7
(Ni)	Cu	cF4	Fm-3 m	7
(Zr)ht	W	cI2	Im-3 m	7
$\tau_1(Zr_{65}Mo_{18-x}Ni_{16.5+x})$ $0 \le x \le 2.5$	Ti_2Ni	cF96	Fd-3 m	8
$\tau_2(Zr_{65}Mo_{27.3}Ni_{7.7})$	Hf_9Mo_4B	hP28	$P6_3/mmc$	9

with the Ni_5Zr and Ni_7Zr_2 by Virkar et al.,[14] while the equilibrium suggested by Prima et al.[15–17] was (Ni), Ni_5Zr and Ni_7Zr_2. Thus, the phase relationship among (Ni), $MoNi_3$, Ni_5Zr and Ni_7Zr_2 was controversial; (3) the homogeneous range of the (Mo) phase was different among their work.[14–17] A large extension of the (Mo) phase region was suggested by Virkar et al.[14] This feature seems to be incorrect and needs further investigation; and (4) the binary phase Ni_3Zr, which was stable in the assessed binary system,[10] was not found in their work at 900 °C.[14–17]

To clarify the above contradictions on the phase equilibria in the Mo-Ni-Zr system and provide new phase diagram data for a future thermodynamic modeling, the present work is intended to investigate the phase equilibria of the Mo-Ni-Zr system at 900 °C experimentally.

2. Experimental Procedure

The pure Mo rods (99.99 wt.%), Ni granules (99.99 wt.%) and Zr rods (99.99 wt.%) were used as starting materials. Eighteen Mo-Ni-Zr samples covering the whole composition range were prepared. The alloy samples with the mass of about 2 g were prepared by arc-melting in an arc furnace under high purity argon atmosphere (WKDHL-1, Opto-electronics Co, Ltd., Beijing, China). The large difference of melting temperature among Mo, Zr and Ni makes it difficult to prepare homogeneous alloys by direct melting these three components. Thus, Mo and Zr pure metals were melted firstly to prepare master alloys and then melted with Ni. Each alloy was remelted at least four times to improve their homogeneity. The weight loss after melting was less than 0.5 wt.%, indicating that the real compositions of alloys are close to their nominal compositions. The prepared samples were encapsulated in an evacuated silica capsules under vacuum and then annealed at 900 °C in a high-precision diffusion furnace (L4514, Qingdao Institute & Equipment Co. Ltd., China) for 40 days followed by quenching in cold water.

Phase identification was performed by x-ray diffraction (XRD, Bruker D8 Advance, Germany) using a monochromatic Cu Kα (λ = 1.54056 Å) with a LYNXEYE_XE detector at 40 kV and 40 mA. High purity Si (99.999 wt.%) powder was used as an internal standard for the calculations of lattice parameters. Most of the prepared Mo-Ni-Zr alloys are ductile, so the samples had to be filed into fine powders and re-annealed at the previous heat-treatment temperature for 12 h in order to remove the stress of powders and obtain sharp diffraction patterns. Lattice parameters for the identified phases were calculated by using Jade software.[18] The metallographic alloy samples were examined by optical microscopy (Leica DMLP, Germany) and then analyzed by electron probe microanalysis (EPMA, JXA-8230, JEOL, Japan) for microstructure observation and phase composition measurement.

3. Results and Discussion

The nominal compositions of the prepared ternary alloys are listed in Table 2, in which the identified phases, calculated lattice parameters and phase compositions are also presented. The lattice parameters cannot be obtained for a few Ni-Zr binary phases due to their small quantity and poor quality of diffraction patterns. The typical Back-scattering electron (BSE) images of Mo-Ni-Zr samples are shown in Fig. 2(a)-(f), while the selected XRD patterns for Mo-Ni-Zr alloys are shown in Fig. 3(a)-(f). Based on the present experimental work, the isothermal section of the

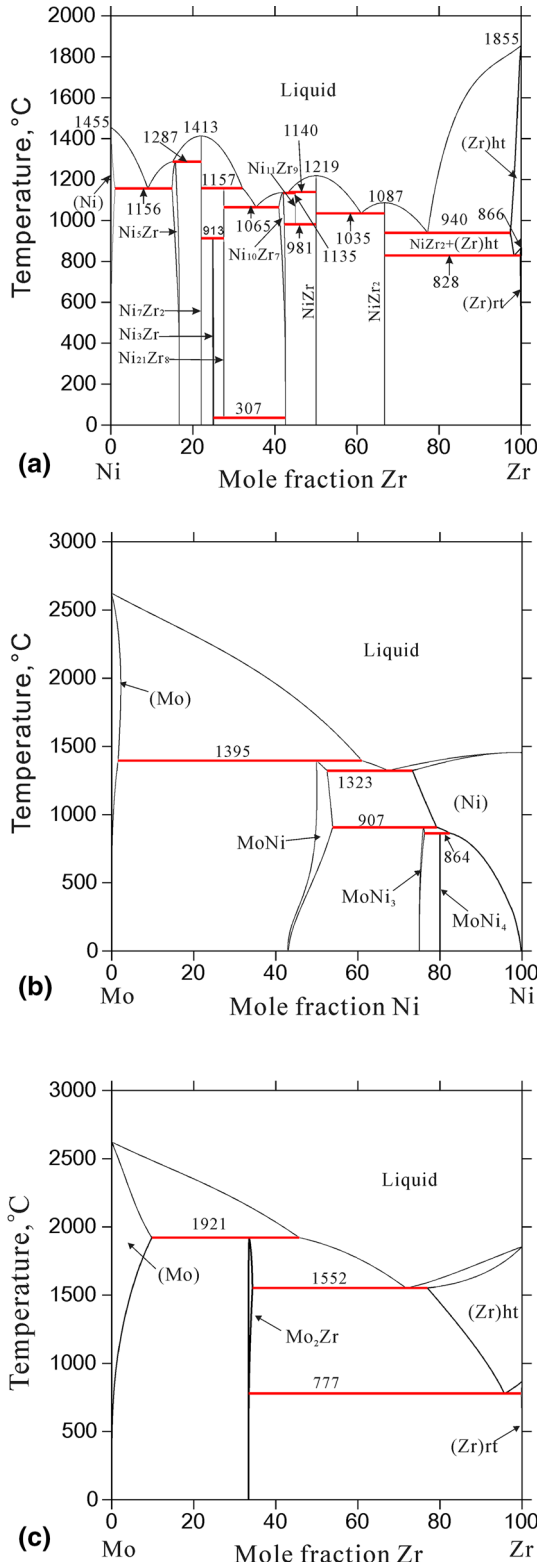

Fig. 1 (a) The calculated Ni-Zr phase diagram according to Tokunaga et al.[10] (b) The calculated Mo-Ni phase diagram based on the optimization by Santhy et al.[11] (c) The calculated Mo-Zr phase diagram according to Pérez et al.[12]

Mo-Ni-Zr system at 900 °C is constructed and presented in Fig. 4, together with the nominal compositions of the prepared samples.

According to the XRD and EPMA results, samples 1, 3-9 and 11-15 are located in three-phase regions. Thirteen three-phase regions were observed in the present work: (1) (Ni) + Ni_7Zr_2 + Ni_5Zr, (2) MoNi + $MoNi_3$ + Ni_7Zr_2, (3) Ni_7Zr_2 + MoNi + (Mo), (4) (Mo) + Ni_7Zr_2 + Ni_3Zr, (5) (Mo) + Ni_3Zr + $Ni_{21}Zr_8$, (6) (Mo) + $Ni_{21}Zr_8$ + $Ni_{10}Zr_7$, (7) (Mo) + $Ni_{10}Zr_7$ + NiZr, (8) (Mo) + Mo_2Zr + NiZr, (9) $NiZr_2$ + Mo_2Zr + τ_1, (10) τ_1 + Mo_2Zr + τ_2, (11) τ_2 + Mo_2Zr + (Zr)ht, (12) $NiZr_2$ + τ_1 + (Zr)ht and (13) τ_1 + τ_2 + (Zr)ht.

In Ni-rich corner, the exact compositions of Ni_7Zr_2 phase in the three-phase equilibria (Ni) + $MoNi_3$ + Ni_7Zr_2 were not determined, and thus the tie-triangle in Fig. 4 is presented as dotted line. The reason is due to the small quantity of Ni_7Zr_2 phase in sample 2. We proposed the tie-triangle containing (Ni), $MoNi_3$ and Ni_7Zr_2 to be stable at 900°C mainly on the basis of the three phases observed for alloys 1,3 and 4 (see Fig. 2a).

Among the Ni-Zr binary phases, Ni_3Zr shows instability at a slightly higher temperature above 900 °C.[10] The XRD patterns of samples 5 and 6 show the very weak peaks of Ni_3Zr phase and the equilibria of those regions were mainly constructed based on EPMA results (see Fig. 2b).

In sample 7, a metastable binary phase Ni_2Zr was found, which was reported as a ternary phase $Zr_{33.3}Mo_3Ni_{63.7}$ by Virkar et al.[14] However, Bsenko[19] confirmed it to be an oxygen stabilized product. In this work, the metastable binary phase was detected by XRD, but the results of EPMA show that only three phases, (Mo), $Ni_{21}Zr_8$ and $Ni_{10}Zr_7$, were observed in sample 7 (see Fig. 2c). Furthermore, the binary phases $Ni_{21}Zr_8$ and $Ni_{10}Zr_7$ were found in bulk x-ray diffraction (see Fig. 3b) but not in the powder x-ray diffraction. The results from XRD pattern of bulk sample is preferable due to the short time exposed on air. Based on the above discussions, the tie-triangle of (Mo) + $Ni_{21}Zr_8$ + $Ni_{10}Zr_7$ was established.

In the present work, for alloys whose compositions lie in the ternary triangle region edged by Mo_2Zr, $NiZr_2$ and NiZr often show the coexistence of more than three phases (see sample 10, Fig. 2d). The $NiZr_2$ metastable phase with Fd-3 m structure was found in the XRD pattern of sample 10 (see sample 10, Fig. 3e), which is not a stable phase in the Ni-Zr binary side. According to XRD and EPMA results, the phase relationship of sample 10 with four phases, Mo_2Zr, NiZr, $NiZr_2$ with Fd-3 m structure, and $NiZr_2$ with I4/mcm structure, was confirmed. It was found that these two $NiZr_2$ phase dissolve different amounts of Mo which are 13.58 and 1.15 at.% respectively and contain same quantity of Zr. Based on the results of other samples (i.e. sample 11), the large solubility of Mo in $NiZr_2$ with Fd-3 m structure is abnormal. It is worth noting that the τ_1 ternary phase has the same structure and the analogous composition as metastable $NiZr_2$ phases, which are $Zr_{65}Mo_{18-x}Ni_{16.5+x}$ and $Zr_{65}Mo_{13.58}Ni_{21.42}$ correspond to τ_1 and metastable $NiZr_2$ phase, respectively. Besides, the influence

Table 2 Summary of the XRD and EPMA experimental results of the Mo-Ni-Zr alloys annealed at 900°C for 40 days

	Nominal composition, at.%				Phase composition, at.%			
No.	Zr	Ni	Mo	Phase analysis	Zr	Ni	Mo	Lattice parameter, Å
1	16.5	80	3.5	(Ni)	1.00	83.60	15.40	a = 3.583(9)
				Ni_7Zr_2	19.61	78.69	1.70	a = 4.67(0), b = 8.17(1), c = 12.1(2), β = 95.(2)
				Ni_5Zr	15.42	83.88	0.69	a = 6.704(8)
2	2.5	77.5	20	(Ni)	0.39	82.08	17.53	a = 3.603(8)
				$MoNi_3$	1.47	76.52	22.02	a = 5.07(4), b = 4.22(3), c = 4.45(6)
				Ni_7Zr_2	…(a)	…	…	…(b)
3	11	69	20	MoNi	1.07	51.96	46.96	a = 9.1(1), b = 9.11(5), c = 8.8(6)
				$MoNi_3$	2.01	75.97	22.02	a = 5.06(6), b = 4.23(5), c = 4.46(5)
				Ni_7Zr_2	19.92	77.60	2.48	a = 4.71(4), b = 8.24(7), c = 12.20(7), β = 95.9(8)
4	5	45	50	Ni_7Zr_2	20.17	77.46	2.36	a = 4.70(8), b = 8.22(8), c = 12.22(6), β = 96.0(4)
				MoNi	0.63	47.34	52.03	a = 9.05(3), b = 9.19(8), c = 8.76(2)
				(Mo)	0.48	3.70	95.82	a = 3.141(7)
5	18.6	61.4	20	(Mo)	0.17	4.55	95.29	a = 3.1470(8)
				Ni_7Zr_2	22.40	77.54	0.06	a = 4.657(6), b = 8.22(1), c = 12.27(0), β = 96.6(9)
				Ni_3Zr	25.10	74.83	0.08	…(b)
6	19	61	20	(Mo)	0.50	3.25	96.25	a = 3.146(6)
				Ni_3Zr	25.51	74.42	0.08	…(b)
				$Ni_{21}Zr_8$	27.54	72.36	0.10	…(b)
7	27	53	20	(Mo)	0.91	5.22	93.87	a = 3.147(4)
				$Ni_{21}Zr_8$	28.94	70.65	0.40	…(b)
				$Ni_{10}Zr_7$	39.25	60.55	0.20	…(b)
8	37	43	20	(Mo)	3.58	2.08	94.33	a = 3.156(1)
				$Ni_{10}Zr_7$	42.37	57.47	0.15	a = 12.32(4), b = 9.20(7), c = 9.20(9)
				NiZr	50.72	49.13	0.15	a = 3.296(7), b = 10.01(9), c = 4.06(3)
9	30	20	50	NiZr	50.18	48.98	0.84	a = 3.27(4), b = 9.8(8), c = 4.1(1)
				(Mo)	6.94	1.00	92.06	a = 3.165(0)
				Mo_2Zr	34.05	2.65	63.30	a = 7.575(7)
10	50	30	20	Mo_2Zr	33.82	3.98	62.20	a = 7.579(5)
				$NiZr_2$	65.14	33.71	1.15	…(b)
				NiZr	49.40	50.57	0.04	a = 3.29(2), b = 9.9(7), c = 4.09(7)
11	60	20	20	Mo_2Zr	35.48	2.14	62.38	a = 7.582(0)
				$NiZr_2$	67.94	31.39	0.67	a = 6.4(8), c = 5.2(7)
				τ_1	64.83	17.00	18.17	a = 12.34(1)
12	60.73	10.47	28.8	Mo_2Zr	35.13	0.79	64.07	a = 7.58(6)
				τ_2	64.72	7.81	27.47	a = 8.74(6), c = 8.54(5)
				τ_1	64.04	16.54	19.42	a = 12.360(6)
13	67.9	3.8	28.3	Mo_2Zr	35.34	0.52	64.14	a = 7.603(4)
				(Zr)ht	89.57	0.75	9.68	a = 3.560(5)
				τ_2	64.59	7.33	28.08	a = 8.71(6), c = 8.57(3)
14	73.9	18.8	7.3	$NiZr_2$	66.76	32.68	0.57	a = 6.48(3), c = 5.27(3)
				τ_1	65.65	18.86	15.49	a = 12.339(8)
				(Zr)ht	91.39	1.48	7.14	a = 3.554(1)
15	70	10	20	(Zr)ht	90.73	1.37	7.90	a = 3.568(2)
				τ_2	65.81	7.88	26.31	a = 8.74(3), c = 8.52(1)
				τ_1	65.32	16.46	18.22	a = 12.34(7)
16	5	90	5	(Ni)	0.04	93.31	6.66	…(b)
				Ni_5Zr	16.50	83.18	0.32	…(b)
17	4	85	11	(Ni)	0.26	85.81	13.94	…(b)
				Ni_5Zr	16.38	83.02	0.61	…(b)
18	65.67	7.76	26.57	τ_2	64.90	7.51	27.59	a = 8.753(1), c = 8.508(7)

(a) Due to the small amount of the phase, the phase composition cannot be determined accurately

(b) The lattice parameters were not calculated due to the small quantity of these phases or the poor quality of diffraction patterns

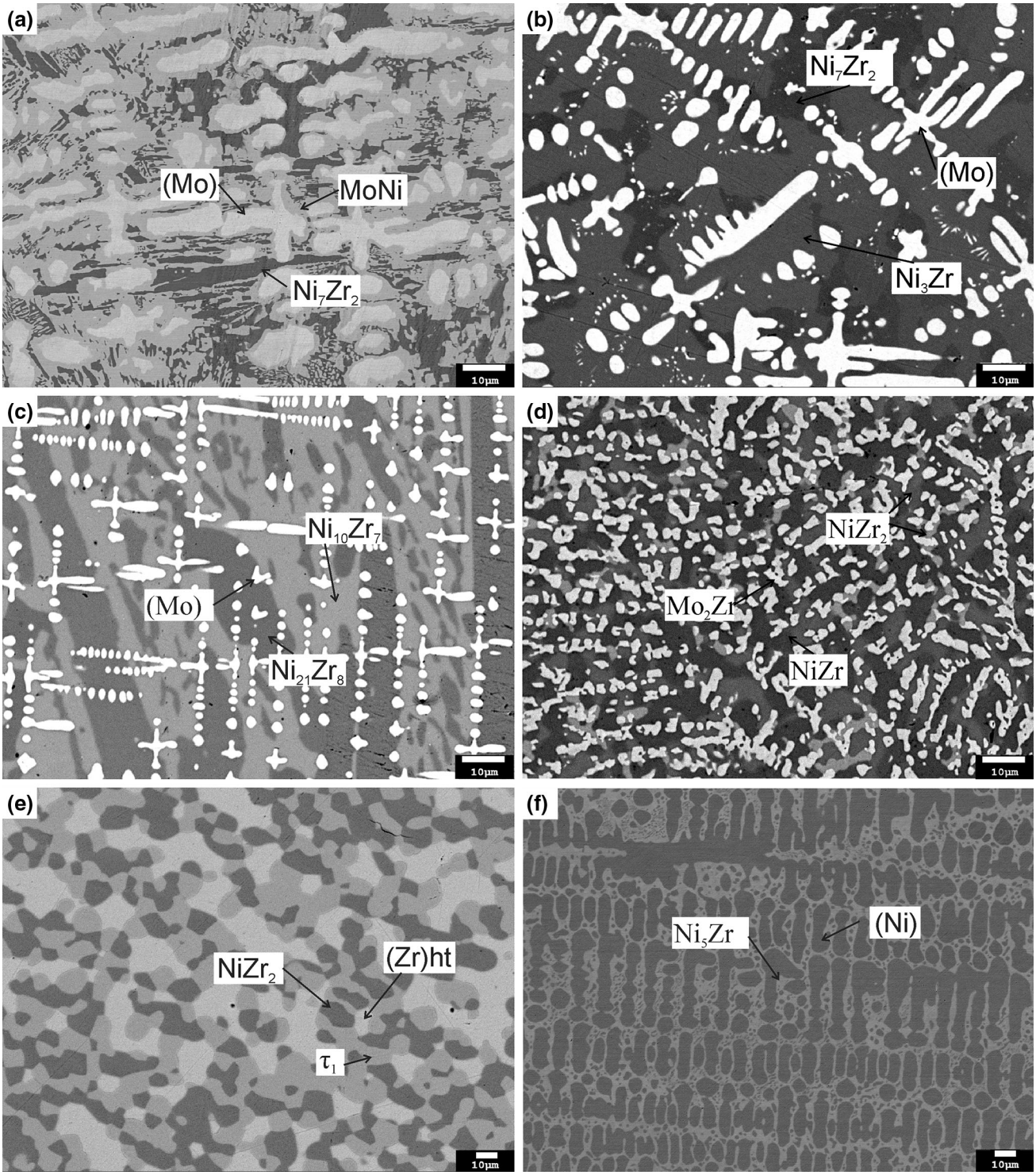

Fig. 2 BSE images of typical Mo-Ni-Zr ternary alloys annealed at 900 °C(at.%): (a) Annealed alloy $Mo_{50}Ni_{45}Zr_5$, (b) Annealed alloy $Mo_{20}Ni_{61.4}Zr_{18.6}$, (c) Annealed alloy $Mo_{20}Ni_{53}Zr_{27}$, (d) Annealed alloy $Mo_{20}Ni_{30}Zr_{50}$, (e) Annealed alloy $Mo_{7.3}Ni_{18.8}Zr_{73.9}$ and (f) Annealed alloy $Mo_5Ni_{90}Zr_5$

of oxygen and other impurities (such as B) on the formation of the metastable $NiZr_2$ was confirmed by Altounianet al.[20] However, several investigations reported by Cacciamani et al.[21,22] in Ni-Zr and B-Ni-Zr system did not indicate any ternary phases corresponding to the metastable $NiZr_2$ on the Zr-rich corner. Moreover, three complementary alloys,

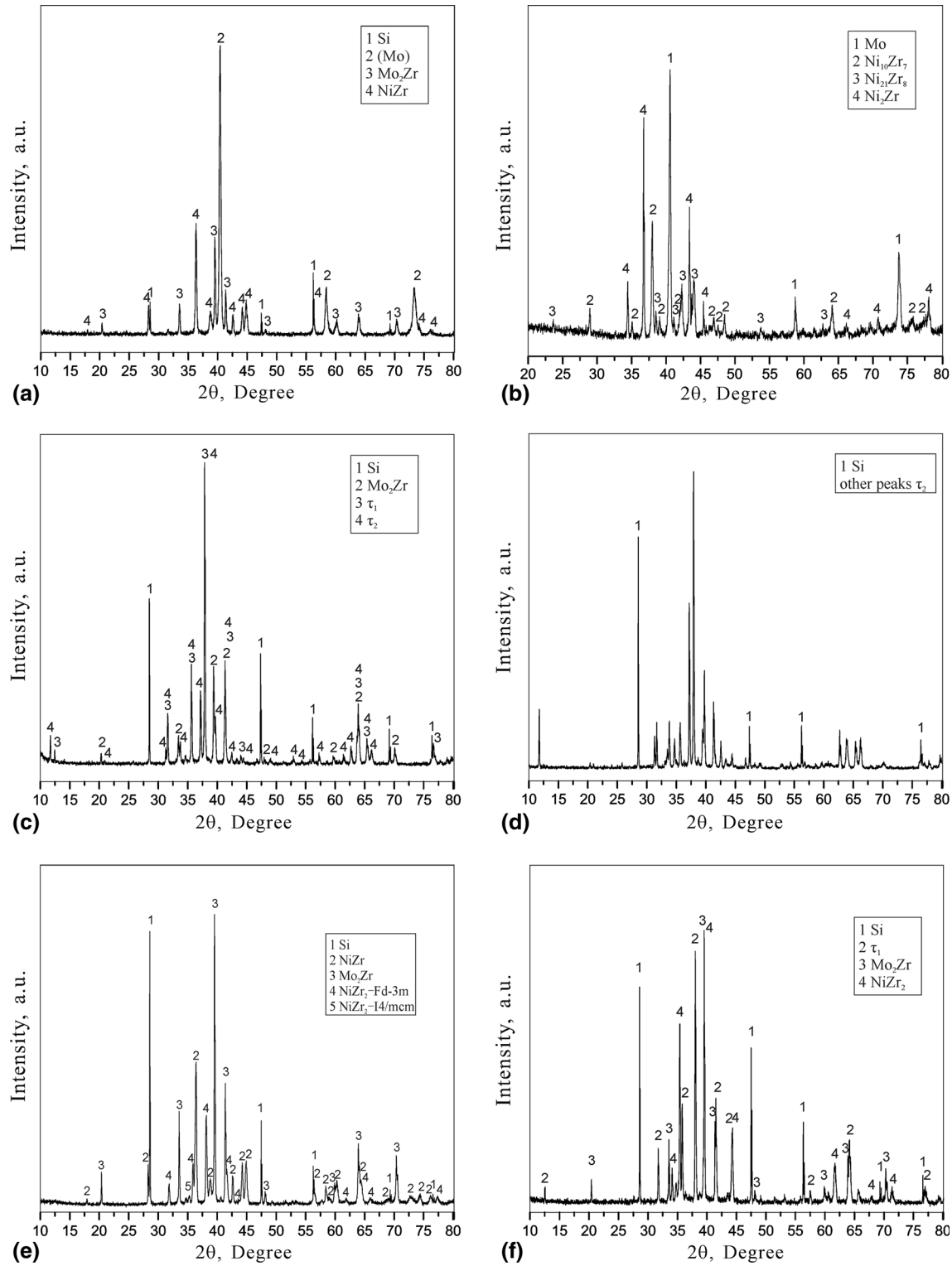

Fig. 3 XRD patterns of typical Mo-Ni-Zr ternary alloys annealed at 900 °C(at.%): (a) Annealed alloy $Mo_{50}Ni_{20}Zr_{30}$, (b) Annealed alloy $Mo_{20}Ni_{53}Zr_{27}$, (c) Annealed alloy $Mo_{28.8}Ni_{10.47}Zr_{60.73}$, (d) Annealed alloy $Mo_{26.57}Ni_{7.76}Zr_{65.67}$, (e) Annealed alloy $Mo_{20}Ni_{30}Zr_{50}$ and (f) Annealed alloy $Mo_{20}Ni_{20}Zr_{60}$

which have the same composition as sample 10, were prepared and annealed at 900 °C for different annealing times (30, 40 and 50 days). However, the identical phase relationship was found as in sample 10. The above conclusions indicating that the existence of the metastable $NiZr_2$ phase is probably caused by oxygen

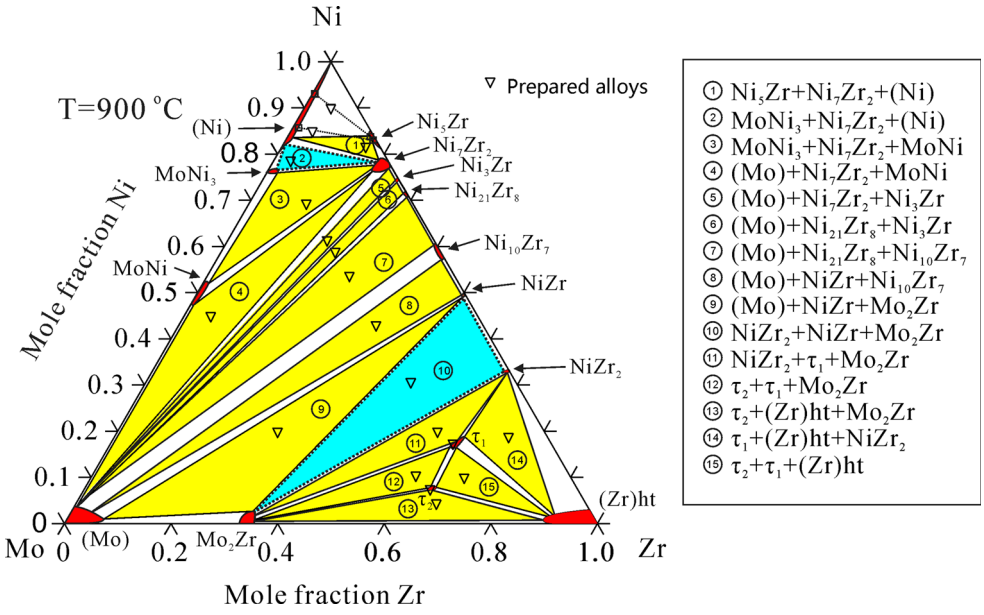

Fig. 4 The constructed isothermal section of the Mo-Ni-Zr system at 900 °C according to the present experimental determinations

impurity and the existence of Mo. Nevertheless, the essential reason for the formation of the metastable $NiZr_2$ phase is still unclear and needs further investigations.

In the presently investigated Mo-Ni-Zr isothermal section, a few binary phases dissolve appreciable amounts of the third component. For example, the maximum solubility of Zr in $MoNi_3$ was determined to be 2.01 at.% Zr. The solubilities of Ni in Mo_2Zr and Mo in Ni_7Zr_2 were measured to be 3.98 at.% Ni and 2.48 at.% Mo, respectively.

In the Zr-rich corner, two ternary compounds (τ_1 and τ_2) were detected, together with their crystal structure, cF96-Ti_2Ni and hP28-Hf_9Mo_4B, respectively. Based on the EPMA results on several alloys containing the τ_1 phase (see also sample 14, Fig. 2e), a homogeneity region extending along the ~65 at.% Zr concentration line was established, leading to the general formula $Zr_{65}Mo_{18-x}Ni_{16.5+x}$ ($0 \le x \le 2.5$) for τ_1. The lattice parameter calculated for $x = 2.5$ is lower than that for $x = 0$ (see Table 2), which is consistent with the feature that the atomic radius of Ni is smaller than that of Mo. The solubility range of τ_2 is negligible, and the stoichiometric composition of τ_2 was determined to be $Zr_{65}Mo_{27.3}Ni_{7.7}$.

In the Ni-rich corner, a two-phase region constructed by (Ni) and Ni_5Zr was confirmed (Fig. 2f). The solubility of Zr in (Ni) is low, and it was measured to be less than 1.0 at.% Zr.

4. Conclusions

The phase equilibria of the Mo-Ni-Zr system have been systematically investigated via XRD analysis and EPMA measurement, and the 900 °C isothermal section of the Mo-Ni-Zr system was established. The major feature of the three-phase equilibria involves the binary solution phases and two ternary compounds $Zr_{65}Mo_{18-x}Ni_{16.5+x}$ (τ_1, $0 \le x \le 2.5$, cF96-Ti_2Ni) and $Zr_{65}Mo_{27.3}Ni_{7.7}$ (τ_2, hP28-Hf_9Mo_4B).

Thirteen three-phase equilibria at 900 °C were well determined. In the present system, a few binary phases dissolve appreciable amounts of the third component. For instance, the maximum solubility of Zr in $MoNi_3$ was determined to be 2.01 at.%. The solubility of Ni in Mo_2Zr and Mo in Ni_7Zr_2 were measured to be 3.98 at.% Ni and 2.48 at.% Mo, respectively.

The four contradictions previously mentioned are clarified and summarized as follows: (1) the existence of the two ternary compounds $Zr_{65}Mo_{18-x}Ni_{16.5+x}$ (τ_1, $0 \le x \le 2.5$, cF96-Ti_2Ni) and $Zr_{65}Mo_{27.3}Ni_{7.7}$ (τ_2, hP28-Hf_9Mo_4B) was confirmed; (2) in the Ni-rich corner, the three-phase equilibria of (Ni) + Ni_5Zr + Ni_7Zr_2 were determined; (3) the maximum solubility of the (Mo) phase was identified as 6.94 at.% Zr and 5.22 at.% Ni; and (4) the Ni_3Zr binary phase was found at 900 °C in this work.

The presently developed phase equilibria of the Mo-Ni-Zr system at 900 °C can provide new phase diagram data for thermodynamic optimization of the Mo-Ni-Zr system.

Acknowledgments

The financial supports from the National Natural Science Foundation of China (Grant No. 51371199), Ministry of Industry and Information Technology of China (Grant No. 2015ZX04005008) and Project of Innovation-driven Plan in Central South University (Grant No. 2015CX004) are greatly acknowledged.

References

1. P. Ettmayer, H. Kolaska, W. Lengauer, and K. Dreyer, Ti(C, N) Cermets—Metallurgy and Properties, *Int. J. Refract. Met. Hard Mater.*, 1995, **13**(6), p 343-351
2. J. Zackrisson and H.-O. Andrén, Effect of Carbon Content on the Microstructure and Mechanical Properties of (Ti, W, Ta, Mo)(C, N)-(Co, Ni) Cermets, *Int. J. Refract. Met. Hard Mater.*, 1999, **17**(4), p 265-273
3. Y. Li, N. Liu, X. Zhang, and C. Rong, Effect of Mo Addition on the Microstructure and Mechanical Properties of Ultra-Fine Grade TiC-TiN-WC-Mo_2C-Co Cermets, *Int. J. Refract. Met. Hard Mater.*, 2008, **26**(3), p 190-196
4. X. Zhang, N. Liu, C. Rong, and J. Zhou, Microstructure and Mechanical Properties of TiC-TiN-Zr-WC-Ni-Co Cermets, *Ceram. Int.*, 2009, **35**(3), p 1187-1193
5. X. Zhang and N. Liu, Effects of ZrC on Microstructure, Mechanical Properties and Thermal Shock Resistance of TiC-ZrC-Co-Ni Cermets, *Mater. Sci. Eng., A*, 2013, **561**, p 270-276
6. M.H. Yang, S.N. Li, Y. Li, J.H. Li, and B.X. Liu, Atomistic Modeling to Optimize Composition and Characterize Structure of Ni-Zr-Mo Metallic Glasses, *Phys. Chem. Chem. Phys.*, 2015, **17**(20), p 13355-13365
7. http://materials.springer.com/isp/phase-diagram/docs/c_1301041
8. http://materials.springer.com/isp/crystallographic/docs/sd_0461606
9. http://materials.springer.com/isp/crystallographic/docs/sd_0536140
10. T. Tokunaga, S. Matsumoto, H. Ohtani, and M. Hasebe, Thermodynamic Analysis of the Phase Equilibria in the Nb-Ni-Zr System, *Mater. Trans.*, 2007, **48**(9), p 2263-2271
11. K. Santhy and K.H. Kumar, Thermodynamic Assessment of Mo-Ni-Ti Ternary System by Coupling First-Principle Calculations with CALPHAD Approach, *Intermetallics*, 2010, **18**(9), p 1713-1721
12. R. Jerlerud Pérez and B. Sundman, Thermodynamic Assessment of the Mo-Zr Binary Phase Diagram, *Calphad*, 2003, **27**(3), p 253-262
13. K.P. Gupta, The Mo-Ni-Zr System (Molybdenum-Nickel-Zirconium), *J. Phase Equilib.*, 2000, **21**(1), p 95-101
14. A.V. Virkar and A. Raman, Alloy Chemistry of σ(β-U)-Related Phases. II. Characteristics of δ and Other σ-Related Phases in Some Mo-NiX Systems, *Z. MetaIlkd.*, 1969, **60**(7), p 594-600
15. S.B. Prima, N.V. Dan'ko, and V.M. Petyukh, Phase Equilibria in the Nickel-Zirconium-Molybdenum System at Subsolidus Temperatures and 900 °C, *Izv. Vyssh. Uchebn. Zaved. TsvetnMetall.*, 1991, **3**, p 86-94
16. S.B. Prima and V.M. Petyukh, Phase Relations in Solidification of Nickel-Zirconium-Molybdenum Alloys in the ZrNi-Ni-Mo Region, *Metally*, 1991, **6**, p 161-167
17. S.B. Prima and V.M. Petyukh, Phase Transformations During Solidification of Nickel-Zirconium-Molybdenum Alloys in the Zr-ZrNi-Mo Region, *Metally*, 1993, **5**, p 205-212
18. JADE 6.0, Users Guide for XRD Pattern Processing. In: Materials Data I, (Ed.). CA, USA, 2005
19. L. Bsenko, The Hafnium-Nickel and Zirconium-Nickel Systems in the Region 65-80 at.% Nickel, *J. Less-Common Met.*, 1979, **63**(2), p 171-179
20. Z. Altounian, E. Batalla, J.O. Strom-Olsen, and J.L. Walter, The Influence of Oxygen and Other Impurities on the Crystallization of NiZr2 and Related Metallic Glasse, *J. Appl. Phys.*, 1987, **61**(1), p 149
21. G. Cacciamani, P. Riani, and F. Valenza, Equilibrium Between MB2 (M = Ti, Zr, Hf) UHTC and Ni: A Thermodynamic Database for the B-Hf-Ni-Ti-Zr System, *Calphad*, 2011, **35**(4), p 601-619
22. F. Valenza, M.L. Muolo, A. Passerone, G. Cacciamani, and C. Artini, Control of Interfacial Reactivity Between ZrB2 and Ni-Based Brazing Alloys, *J. Mater. Eng. Perform.*, 2012, **21**(5), p 660-666